Experimental evaluation of aquatic ecosystem resistance and resilience to episodic nutrient loading

Tyler J. Butts[1,2*], Robert A. Johnson[1,3], Michael J. Weber[4], Grace M. Wilkinson[1,2,3]

[1]Department of Ecology, Evolution, and Organismal Biology, Iowa State University, Ames, IA, USA

[2]Present Address: Center for Limnology, University of Wisconsin-Madison, WI, USA

[3]Present Address: Department of Integrative Biology, University of Wisconsin-Madison, Madison, WI, USA

[4]Department of Natural Resource Ecology and Management, Iowa State University, Ames, IA, USA

* Corresponding author: Tyler J. Butts, email: tjbutts@wisc.edu

Open research statement: Data will be archived through the Environmental Data Initiative and given a unique digital object identifier. Scripts for data analysis and figure generation are available at https://github.com/tjbutts/hort-benthic-pelagic, including the data for review, and will be archived through Zenodo upon acceptance.

Keywords/phrases: pulse perturbation; benthic-pelagic coupling; resistance; resilience; food web structure; phytoplankton; shallow lakes; experimental ponds

ABSTRACT

The frequency and intensity of ecosystem disturbances is increasing due to climate change. However, the structure of trophic interactions within food webs may mediate the resistance and resilience of ecosystems to disturbance events. In aquatic ecosystems, high connectivity between benthic and pelagic food chains (i.e., benthic-pelagic coupling) is theorized to generate more pathways for nutrients and energy to flow as well as strengthen top-down control. As such, we predicted that greater benthic-pelagic coupling would increase the resistance (longer response time) and resilience (shorter recovery time) of aquatic primary production to pulse disturbances and reduce the chance of a critical transition. To test this prediction, we simulated two storm-induced pulse disturbances by adding N and P (~3% and ~5% increase in ambient concentrations) to three experimental ponds with food webs containing low, intermediate, and high benthic-pelagic coupling. Another set of ponds with matching food web structures served as reference ecosystems. We evaluated the primary production response time (resistance) and recovery time (resilience) following each nutrient pulse using a response detection algorithm and quantified the occurrence of a critical transition in algal biomass. The high coupling pond never exceeded the response threshold. Following our prediction, chlorophyll-*a* concentrations exceeded the response threshold after 18 and 24 days in the intermediate and low coupling ponds, respectively. There was also evidence of a critical transition in the low coupling pond following the first pulse. After the second nutrient pulse, chlorophyll-*a* exceeded the response threshold again in both low and intermediate ponds, but the response was much faster in the low coupling pond (8 days) compared to the intermediate coupling pond (20 days), though again there was no response in the high coupling pond. Recovery time increased substantially after the second pulse in the low coupling pond increasing from 8 to 22 days and did not occur following the second pulse in the intermediate pond.

Together, these results support our prediction that greater benthic-pelagic coupling confers greater resistance and resilience to repeated pulses of nutrient loading, demonstrating that food web structure can mediate ecosystem responses to disturbance.

INTRODUCTION

The frequency, scale, and intensity of ecosystem disturbances are increasing as accelerating climate change drives more frequent and intense temperature extremes and precipitation (Seneviratne et al. 2021). Changes to disturbance regimes driven by climate change are also increasing the likelihood of abrupt changes, rapid shifts in ecosystem state relative to typical rates of change within the ecosystem (Turner et al. 2020). For example, extreme heat waves have been linked to mass bleaching events in coral reefs (Hughes et al. 2018) and extreme precipitation, along with agricultural land use, has been tied to increased eutrophication and higher abundances of toxin-producing phytoplankton in aquatic ecosystems (Ho and Michalak 2020). Abrupt changes can also become critical transitions, a transition from one equilibrium state to another, which may prevent ecosystem recovery to the prior state and increased vulnerability to further disturbances (Scheffer and Carpenter 2003, Taranu et al. 2018). Understanding the mechanisms mediating effects of disturbance on ecosystem function is imperative for effective ecosystem management in the face of global change.

Pulse disturbances, sudden and temporally constrained disturbances that alter biomass or composition of ecological communities, are ubiquitous in aquatic ecosystems and expected to increase (Prein et al. 2017). For example, large precipitation events, which are increasing in frequency and magnitude in some regions (Seneviratne et al. 2021), deliver pulses of nitrogen (N) and phosphorus (P) to surface waters (Joosse and Baker 2011). In many lakes, annual

nutrient loading is disproportionately dominated by a few loading events during large storms (Carpenter et al. 2018). In agricultural watersheds, inputs of P from fertilizer and manure to the landscape exceed crop uptake by 50% in some areas, generating surplus P that is readily mobilized (Sabo et al. 2021). Excess nutrients fuel eutrophication resulting in increasing turbidity, depleted dissolved oxygen, and proliferation of toxin-producing phytoplankton that adversely affect human health (Carmichael and Boyer 2016). However, not all lakes will respond to nutrient pulses in the same way as antecedent conditions, ecosystem properties, and watershed characteristics affect whether nutrient pulses linked to storm events will alter ecosystem function or trigger an abrupt change (Stockwell et al. 2020). Thus, there is a pressing need to better understand the mechanisms that mediate aquatic ecosystem responses to pulse nutrient disturbances.

The strength of interactions between species and overall food web architecture plays a critical role in determining how ecological communities will react to increasing and interacting disturbances (McCann et al. 1998, Polazzo et al. 2022). Food web structure can produce differences in the resistance (defined here as the response time and response magnitude to the nutrient pulse) and resilience (defined here as the rate at which the system recovered from the nutrient pulse) of aquatic ecosystems to nutrient additions (Cottingham and Schindler 2000). For example, during a whole-ecosystem nutrient pulse experiment in two small lakes in northern Wisconsin, increasing the number of trophic levels from two to three through the addition of a planktivore led to decreased ecosystem resistance to nutrient pulses (Cottingham and Schindler 2000). Other components of food web structure (e.g., connectivity, structural asymmetry, functional diversity) may also alter the ability of aquatic ecosystems to mitigate the effects of disturbances (Calizza et al. 2019, Wojcik et al. 2021). For example, the coupling of the algae-

based food chain to the detritus/periphyton-based food chain by generalist consumers (Vadeboncoeur et al. 2002, Vander Zanden and Vadeboncoeur 2002) is a common food web architecture in lakes (hereafter benthic-pelagic coupling).

Benthic-pelagic coupling is theorized to improve ecosystem resilience to complex and interacting disturbances by increasing connectivity and modularity within food webs which provides stability in the face of changing resource availability (McMeans et al. 2016). There is a mix of empirical and theoretical evidence that benthic-pelagic coupling can strengthen aquatic trophic cascades by providing resource subsidies and higher growth potential for top consumers in the food chain (Vadeboncoeur et al. 2005, Vander Zanden et al. 2005). Furthermore, benthic-pelagic coupling may influence ecosystem stability, resilience, and nutrient cycling (Rooney and McCann 2012, Baustian et al. 2014). Such mechanisms may reduce the occurrence of abrupt changes or even critical transitions within aquatic ecosystems. While benthic-pelagic coupling in food webs is theorized to significantly influence ecosystem responses to disturbances, there is limited empirical evidence demonstrating how, and to what degree, benthic-pelagic coupling affects resistance and resilience to nutrient pulses.

We performed a set of whole-ecosystem manipulations to empirically evaluate if the degree of benthic-pelagic coupling affects ecosystem responses to pulse nutrient loading events. Specifically, we asked (1) does the degree of benthic-pelagic coupling affect the response and recovery time of primary production to nutrient pulses? and (2) does the degree of benthic-pelagic coupling influence whether a critical transition occurs in response to a pulse nutrient loading event? We predicted that greater benthic-pelagic coupling would result in slower response times of primary production to nutrient pulses (i.e., greater resistance), faster return times (i.e., greater resilience), and a reduced chance of a critical transition occurring due to

stronger top-down control and the presence of more pathways by which energy and nutrients could flow within the food web. To address these questions, we performed a series of paired ecosystem experiments in ponds with food web structures that varied in benthic-pelagic coupling subjecting one pond in each pair to two nutrient pulse disturbances.

METHODS

The experiment occurred in summer 2020 at the Iowa State Horticultural Research Station (42.110005, -93.580454) in a set of six experimental ponds. The ponds have a wetted surface area of roughly 400 m^2 and a mean depth of 0.8 m (maximum: 2 m). The ponds' watersheds were limited to a few meters on each side and the bottom was sealed with bentonite clay to restrict groundwater flow. The only hydrologic input during the experiment was direct precipitation. In April 2020, the ponds were filled with water from the on-site irrigation reservoir seeding each pond with a similar assemblage of phytoplankton and zooplankton. Communities of emergent longleaf pondweed (*Potamogeton nodosus*) and submerged leafy pondweed (*Potamogeton foliosus*) were naturally established in each pond.

Experimental Design

Three fish assemblages were established in the six ponds to create food web structures with low, intermediate, and high trophic connectivity between benthic and pelagic food chains (Figure 1). Each fish assemblage was randomly assigned to two ponds that were paired in the experiment with one receiving the pulse nutrient additions (see description below) and one serving as an unmanipulated reference. The ponds with the lowest number of trophic connections between benthic and pelagic food chains (hereafter, low benthic-pelagic coupling) consisted of

142 planktivorous bluegill (*Lepomis macrochirus,* Werner and Hall 1988), zooplankton, and
143 phytoplankton in the pelagic pathway and zoobenthivorous yellow perch (*Perca flavescens*,
144 Tyson and Knight 2001), macroinvertebrates, periphyton, and detritus in the benthic pathway.
145 Ponds with slightly more trophic connections between benthic and pelagic food chains (hereafter,
146 intermediate benthic-pelagic coupling) had the same assemblage as the low coupling ponds in
147 addition to a generalist consumer, largemouth bass (*Micropterus salmoides*), which preys in both
148 benthic and pelagic food chains (Hodgson and Hodgson 2000). The ponds with the highest
149 number of trophic connections between benthic and pelagic food chains (hereafter, high benthic-
150 pelagic coupling) consisted of the same assemblage as the intermediate coupling ponds with an
151 additional generalist consumer, fathead minnows (*Pimephales promelas*, Duffy 1998).
152 Fish biomass for each species was kept consistent across ponds (Table 1). For example,
153 the biomass of bluegill added to one pond was the same biomass added to all the other ponds.
154 When a pond had an additional species, such as the intermediate and high coupling ponds, we
155 kept the biomass of species consistent across ponds, but total fish biomass increased (i.e., an
156 additive design; Carey and Wahl 2010). The total fish biomass for all ponds (40 – 80 kilograms
157 per hectare, kg ha^{-1}) fell within the range of values reported (28 – 305 kg ha^{-1}) for several North
158 American lakes (Carlander 1977). All fish used to establish the food webs were collected via
159 electrofishing from Brushy Creek Lake (42.39194, -93.98917) except for bluegill which were
160 harvested from both Brushy Creek Lake and Five Island Lake (43.15806, -94.64667). Fathead
161 minnows were purchased from Beemer Fisheries in Bedford, IA. Yellow perch were stocked in
162 all ponds on day of year (DOY) 98 and 99 with additional perch added on DOY 127 to replace
163 individuals that died from stress or natural mortality. Bluegill were added to all ponds on DOY
164 127 and 128 from Brushy Creek Lake and from Five Island Lake on DOY 133. On DOY 141,

largemouth bass were added to both the intermediate and high benthic-pelagic coupling ponds, along with fathead minnows to the high benthic-pelagic coupling ponds.

We performed two discrete nutrient additions (i.e., pulses) to three of the ponds, one from each food web treatment, on DOY 176 and DOY 211 (Figure 1). We designed the nutrient pulses to simulate the magnitude and stoichiometry of a storm-driven nutrient loading event in an agricultural watershed (Vanni et al. 2001, Lürling et al. 2018). The pond volume (~450 m^3) and ambient nutrient concentrations measured the week prior to the planned nutrient pulse additions were used to determine the mass of nitrogen (N) and phosphorus (P) to add (Appendix S1: Table S1) such that the first and second pulses resulted in a 3% and 5% increase in P concentration, respectively. Ambient nutrients were similar across the ponds though P was slightly elevated in the reference ponds compared to the pulsed ponds (Table 1). We added ammonium nitrate (NH_4NO_3) and sodium phosphate monobasic dihydrate ($NaH_2PO4•H_2O$) at a 24N:1P ratio. The nutrients were delivered to the ponds slowly, pouring the N and P mixture dissolved in pond water from a 4 L carboy over the side of a kayak while paddling around the pond for 30 minutes.

Data Collection

Daily data collection began on DOY 142, which was 34 days prior to the first nutrient addition. We collected water samples three times per week from 0.25 m depth to measure concentrations of total and dissolved nutrients. For dissolved nutrients, samples were filtered in the field through Whatman glass fiber filters (0.45 μm), while samples for total nutrients were not filtered. All samples were kept on ice in a cooler before being transported back to the lab, preserved with 100 μL of concentrated sulfuric acid, and stored for later analysis (Appendix S1). To assess the response of primary production to the nutrient pulses, we measured chlorophyll-*a*

concentration, a proxy for phytoplankton biomass, and ecosystem metabolism daily from DOY 142 – 241. Chlorophyll-*a* was measured using a Total Algae Sensor on a YSI Handheld sonde (Yellow Springs Instruments, Yellow Springs, Ohio, USA). The sensor was slowly lowered at a rate of 1 m per 15 s through the water column, continuously logging chlorophyll-*a* concentrations. The mean chlorophyll-*a* value from 0.1-0.3 m depth was used in the statistical analyses (see below). As phytoplankton were not the only primary producers in the ponds, we also measured ecosystem metabolism to quantify the response of all primary producers to the nutrient additions. Dissolved oxygen was recorded every 30 minutes using PME miniDOT loggers (Precision Measurement Engineering, Vista, California, USA) deployed at 0.25 m depth over the deepest point in each pond. An on-site weather station (Onset HOBO U30 USB) provided measurements of photosynthetic active radiation and wind speed.

Rates of gross primary production (GPP), ecosystem respiration (R), and net ecosystem production (NEP) were calculated using the Kalman filter method in the *LakeMetabolizer* package in R (Winslow et al. 2016). Prior to analysis, the DO data were cleaned by removing measurements where DO decreased by more than 2.0 mg L^{-1} from the previous measurement and the subsequent five DO measurements. These sharp declines coincided with water column mixing and erroneously contributed to the metabolism estimates. The gaps were filled through linear interpolation. Of the 576 pond days of dissolved oxygen measurements, no removal and interpolation were necessary for 60% of pond days, only one measurement for 25% of pond days, two measurements for 12.2% of pond days, and three or more measurements per day for 2.8% of pond days. Metabolic rates calculated from free-water oxygen measurements can result in erroneous estimates (i.e., negative GPP, positive R) when physical processes have a stronger effect on DO dynamics than biological processes (Rose et al. 2014). Erroneous metabolism

estimates were removed prior to statistical analysis resulting in 4-7% removed from the low coupling ponds, 12-15% from the intermediate, and 6-18% from the high coupling ponds.

We also monitored biomass of other primary producers including periphyton and consumers including zooplankton, macroinvertebrates, and fish gut content. Periphyton areal biomass was estimated biweekly using modified Hester-Dendy samplers. Zooplankton were sampled twice per week via a 1 m vertical tow of a Wisconsin net (63 μm mesh). Zooplankton crustaceans and rotifers were identified to genus, excluding copepods which were identified to order, and length-mass regressions were used to calculate biomass. Macroinvertebrates were sampled biweekly in the littoral region of each pond using a modified stovepipe sampler (Jackson et al. 2019). Macroinvertebrates were identified using a stereomicroscope to family (mollusks and insects) or class (leeches and oligochaetes). Finally, at the end of the experiment the remaining fish (with the exception of fathead minnows) were collected, and stomach contents were retrieved through gastric lavage. Stomach content samples were identified to the lowest possible taxonomic order using a stereomicroscope. Additional details of sample collection and analysis are in Appendix S1.

Data Analysis

We used the recently developed response detection algorithm (Walter et al. 2022) in the *disturbhf* package in R (Walter and Buelo 2022) to quantify the response and recovery of chlorophyll-*a* and ecosystem metabolism (state variables) to nutrient pulses in each food web treatment. The algorithm calculates the empirical cumulative distribution function (ECDF) for each rolling window of the state variable in the disturbed ecosystem (i.e., the nutrient addition pond) and compares it to the ECDF calculated for the entirety of the state variable time series in

the reference ecosystem (i.e., the reference pond). The maximum difference in the ECDF for each rolling window of the disturbed pond time series is compared to the reference ECDF and expressed as a time series of Z-scores. The Z-score quantifies how far that observation of the difference in ECDFs between the disturbed and reference time series is from the mean of the reference ECDF, expressed in units of standard deviation. We elected to use the entire reference time series rather than an adaptive window as it allowed us to compare the response of the disturbed ecosystem to the total variability expected without any nutrient pulses. We chose a rolling window of seven days for the disturbed ponds to capture rapid changes in primary production following each nutrient pulse. We performed sensitivity analyses using five- and ten-day rolling windows to evaluate the sensitivity of our conclusions to window length and found minimal differences using shorter or longer windows (Table S4). Following Walter et al. (2022), we defined the response time (i.e., resistance) to the nutrient pulses as the number of days after the addition until the Z-score exceeded 2.0. This threshold indicates a significant and rare event that is a substantial departure from reference conditions. Recovery time (i.e., resilience) was defined as the number of days for the Z-score to return to <0.5 following a significant response (Z-score > 2.0). This recovery threshold indicates a return to reference conditions in the disturbed ecosystem.

To identify if, and when, a critical transition occurred within a pond related to the nutrient pulse we used online dynamic linear modeling of the daily chlorophyll-*a* concentration (Taranu et al. 2018). The method requires a complete daily time series and therefore could not be applied to the metabolism estimates due to the removal of days with erroneous estimates. Briefly, this method calculates the eigenvalues of a time series by fitting autoregressive models (AR) with time-varying coefficients (c.f. Ives and Dakos, 2012). Evidence that a critical transition occurred

257 is based on the eigenvalues crossing one from below. A failure of the eigenvalues to cross one
258 from below suggests no critical transition occurred. We fit time-varying AR (p) models to time
259 series of chlorophyll-*a* for each pond with an optimal order of one or two (i.e., lag-1 or lag-2)
260 determined by Akaike's Information Criteria (AICc) model selection (Hurvich and Tsai 1993). If
261 the change in AICc was less than two, both models were considered for evidence of a critical
262 transition (Burnham and Anderson 2004; Appendix S1: Table S2). All analyses were performed
263 in R version 4.2.1 (R Core Team 2022).
264
265 **RESULTS**
266 The different food web structures established within the experimental ponds successfully
267 increased benthic-pelagic coupling (Figure 2). Zooplankton biomass was initially similar across
268 the ponds but diverged after a few weeks (Figure 2A - C). Zooplankton biomass in the low
269 coupling ponds steadily decreased over the summer (Figure 2A), resulting in the lowest mean
270 biomass in this food web treatment (Appendix S1: Figure S1A). In the intermediate and high
271 coupling ponds, zooplankton biomass only modestly declined during the summer (Figure 2A -
272 C), resulting in higher mean biomass in these ponds (Appendix S1: Figure S1B - C).
273 Macroinvertebrate density was variable over time (Figure 2D - F), with the highest densities in
274 the high coupling pond (Figure 2F, Appendix S1: Figure S1D - F). Periphyton areal biomass
275 steadily increased in the pulsed low coupling pond and all reference ponds (Figure 2G - I,
276 Appendix S1: Figure S1G - I). In the low coupling ponds, periphyton biomass remained
277 relatively low (Figure 2). Fish diets collected at the end of the experiment roughly corresponded
278 to our expectations of trophic interactions with bluegill preying on a greater abundance of
279 zooplankton taxa and yellow perch consuming a greater abundance of macroinvertebrate species,

mostly oligochaetes and chironomids (Appendix S1: Table S3). Largemouth bass preyed on a diversity of organisms, but mostly fish and macroinvertebrates (Appendix S1: Table S3). The nutrient pulses did effectively increase ambient nutrients in the pulsed ponds as we observed an increasing trend in nutrient concentrations following each nutrient pulse in comparison to their concentrations prior to nutrient addition (Appendix S1: Figure S2).

Following the first nutrient pulse, chlorophyll-*a* concentration increased and peaked at roughly the same time in both the low (DOY 198) and intermediate (DOY 194) coupling ponds (Figure 3A - B). In comparison, there was no apparent response in chlorophyll-*a* in the high benthic-pelagic coupling pulsed pond (Figure 3C). Following the second nutrient pulse, chlorophyll-*a* concentration increased in all three pulsed ponds with the low coupling pond peaking first on DOY 224, the intermediate coupling pond following on DOY 232, and finally the high coupling pond peaking on DOY 236. Gross primary production (GPP), which encompasses production from all primary producers, was similar to the chlorophyll-*a* dynamics after both nutrient pulses in the intermediate and high coupling ponds but did not follow chlorophyll-*a* dynamics in the low coupling pulsed pond (Figure 3D - F). Respiration (R) steadily increased for all pulsed ponds over the duration of the experiment and followed the reference pond dynamics closely (Figure 3G - I). Net ecosystem production (NEP) initially decreased then remained largely heterotrophic for all ponds following the first nutrient pulse (Figure 3J - L). There was an increase in NEP following the first nutrient pulse in the intermediate coupling pulsed pond akin to the dynamics observed in gross primary production and chlorophyll-*a* (Figure 3H). However, the reference intermediate coupling pond had similar dynamics. The low and intermediate coupling ponds became heterotrophic prior to the first nutrient pulse (between DOY 151 - 172) and remained heterotrophic for the rest of the summer

303 until the end of the experiment (Figure 3J - K). Both the pulsed and reference high coupling
304 ponds remained autotrophic further into the summer than the other two food web structures only
305 becoming heterotrophic on DOY 192 (Figure 3L).

306 We found support for our prediction that the resistance (response time) and resilience
307 (return time) of primary production to the nutrient pulses would be greatest in the high benthic-
308 pelagic coupling pond (Figure 4). Following the first nutrient pulse, the chlorophyll-*a* Z-scores
309 for the low and intermediate coupling ponds surpassed the threshold of 2, indicating a significant
310 response, whereas there was no significant response detected in the high coupling ponds (Figure
311 4A - B). There was also a significant recovery (Z-score of chlorophyll decreased below 0.5) prior
312 to the second nutrient pulse in the low coupling pond, but there was not a significant recovery in
313 the intermediate coupling pond until a few days after the second nutrient pulse. The response
314 time of chlorophyll-*a* in both the low and intermediate coupling ponds to the first nutrient pulse
315 were similar, though the intermediate coupling pond had a longer return time to reference
316 conditions (Table 2). Following the second nutrient pulse, the Z-scores for chlorophyll-*a*
317 concentration again significantly responded in the low and intermediate coupling ponds (Figure
318 4A – C). However, the low coupling pond responded 16 days faster to the second nutrient pulse
319 and took 17 days longer to recover whereas the intermediate coupling pond had a similar
320 response time to the first nutrient pulse, but it did not recover before the experiment was
321 terminated (although the Z-score was trending towards recovery) (Table 2).

322 For GPP, there was only a significant response (Z-score of GPP >2) in the intermediate
323 coupling pond with a seven-day rolling window after both nutrient pulses (Figure 4D – F). GPP
324 in the intermediate coupling pond responded 11 days after the first nutrient pulse and 21 days
325 after the second nutrient pulse. Additionally, GPP in the intermediate coupling pond recovered

(Z-score of GPP<0.5) from the first and second pulses in eleven and five days, respectively (Table 2). There was a significant GPP response detected in the low coupling pond with a shorter rolling window (5-day) on DOY 185 with recovery on DOY 190 (Appendix S1: Figure S3, Table S4). There was no significant response of R or NEP following either nutrient pulse in most of the ponds (Figure 4G – L) except for the intermediate coupling pond where the Z-score of R exceeded the threshold 21 days after the second nutrient pulse, recovering 4 days later (Figure 4H). There was a significant response of R in the high coupling pond early in the time series, but it was before the first nutrient pulse (Figure 4L). With a longer rolling window (10-day) there was a significant response of R in the pulsed high coupling pond 21 days after the second nutrient pulse with no recovery observed as the experiment ended shortly thereafter (Appendix S1: Figure S4, Table S4).

We found some support for our prediction that greater benthic-pelagic coupling would reduce the chance of a critical transition following a nutrient pulse. After the first nutrient pulse, there was only clear evidence of a critical transition in the pulsed low coupling pond where eigenvalues exceeded one from below on DOY 194 and again on DOY 196, 18 to 20 days following the first nutrient pulse (Figure 5A). The timing of the critical transition for chlorophyll-*a* eigenvalues was about two to four days prior to the peak in chlorophyll-*a* concentration observed in the time series (Figure 3) and four to six days prior to the reported significant response based on the response detection algorithm (Figure 4). There was no clear evidence of a critical transition in either the pulsed intermediate or high coupling ponds (Figure 5B – C), nor within any of the reference ponds following the first nutrient pulse (Figure 5D – F). The bootstrapped standard error crossed above one from below in some ponds indicating the potential for a critical transition, but there was no evidence that one occurred following the first

nutrient pulse (Figure 5). There was no evidence of a critical transition in any of the pulsed ponds after the second nutrient pulse, however, there was evidence of a critical transition within the reference low coupling pond on DOY 232 (Figure 5D) and the reference high coupling pond on DOY 241, the last sampling day in autumn (Figure 5F).

DISCUSSION

With this experiment, we established three food web structures that varied in their degree of benthic-pelagic coupling. While food web complexity, the number of trophic guilds, and overall fish biomass increased across the three food web structures, the different dynamics of zooplankton, periphyton, and macroinvertebrates suggests we increased benthic-pelagic coupling between the three established food web structure. There was stronger top-down control on planktivores in the intermediate and high coupling ponds evidenced by higher zooplankton biomass and greater persistence of zooplankton biomass across the summer sampling season, especially within the high coupling pond. In addition, there were larger swings in periphyton and macroinvertebrate biomass akin to standard predator-prey cycles (Blasius et al. 2020) in the high coupling pond, but only partially in the intermediate and low coupling ponds. This indicates a greater reliance on the benthic food chain as benthic-pelagic coupling increased providing evidence our food web treatments were functioning as expected.

In support of our prediction that benthic-pelagic coupling increased ecosystem resistance and resilience to disturbance, there was no response (and therefore, no recovery) of chlorophyll-*a* in the high benthic-pelagic coupling pond to nutrient pulses, whereas there was a response in the low and intermediate coupling ponds. Furthermore, the low coupling pond responded swiftly after the second nutrient pulse in contrast to the intermediate coupling pond which had a similar response time to the first nutrient pulse. While there was a relatively fast recovery in chlorophyll-

372 *a* from the first nutrient pulse in the low coupling pond, there was a far slower recovery
373 following the second nutrient pulse. Additionally, although the intermediate pond did not recover
374 from the second nutrient pulse before the experiment concluded it was on track for a swift
375 recovery. In similar experiments, initially fast recovery from nutrient pulse disturbance has been
376 observed in food webs with higher zooplanktivory (Cottingham and Schindler 2000) as we
377 observed in the low coupling pond. Taken together, the faster response and slower recovery in
378 the low coupling pond after the second nutrient pulse suggests the resistance and resilience to
379 repeated nutrient pulse disturbances only decreased in the low coupling pond.
380 Benthic-pelagic coupling can be a stabilizing force for species within food webs (Mougi
381 2020) which is supported by the lower trophic level dynamics in this experiment. The differences
382 in response and recovery times between the intermediate and high coupling ponds also support
383 our prediction that differences in response were due to stronger top-down control and greater
384 food web connectivity rather than simply a difference in the number of trophic levels (Ward and
385 McCann 2017). With greater benthic-pelagic coupling, there was higher zooplankton biomass,
386 macroinvertebrate density, and periphyton biomass consistent with other studies, likely due to
387 stronger top-down control (Vadeboncoeur et al. 2005, Vander Zanden et al. 2005). However,
388 there may have been an additional refuge effect in the high coupling ponds where the presence of
389 predators led to altered behavior and reduced feeding rates for bluegill, yellow perch, and fathead
390 minnows (Zanette and Clinchy 2019). We only observed a steady decrease in zooplankton
391 biomass in the low coupling ponds indicating that greater benthic-pelagic coupling facilitated
392 more stable zooplankton biomass dynamics. Within the intermediate and high coupling ponds,
393 the cyclical recovery and decline of both macroinvertebrate density and periphyton areal biomass
394 may suggest that fishes were switching to benthivory when macroinvertebrate density was high

allowing periphyton to recover and take up more nutrients with dynamics driven by prey availability.

The dynamics of ecosystem metabolism supported our prediction that greater benthic-pelagic production would reduce the response of primary production to nutrient inputs, though the patterns were far noisier than our chlorophyll-*a* data. There was only a significant response (Z-scores exceeded threshold of 2) in GPP following both nutrient pulses in the intermediate ponds which aligned with the peak in chlorophyll-*a* biomass observed following the first nutrient pulse. Using a smaller rolling window (5 days), GPP significantly responded in the low coupling pond following the first nutrient pulse coinciding with observed chlorophyll-*a* response at the same time. This follows the trophic dynamics we observed within the ponds, indicating phytoplankton production was stimulated under lower top-down control (Cottingham and Schindler 2000). Periphyton was higher in the intermediate coupling ponds in comparison to the low coupling ponds. Thus, the GPP response for the intermediate coupling pond also likely included periphyton (Vadeboncoeur et al. 2001). It is not surprising there were no significant responses for net ecosystem production (NEP) given that it is a balance of GPP and respiration (R); indeed, it had the most stable Z-scores across ponds among all response variables. The complex nature of stratification dynamics, floating leaf macrophytes, and dissolved oxygen changes in the bottom waters of the ponds (Albright et al. 2022), made it difficult to estimate ecosystem metabolism in these ecosystems. Nevertheless, the GPP patterns do support the chlorophyll-*a* dynamics we observed.

There was some support for our prediction that the degree of benthic-pelagic coupling would reduce the chance of a critical transition. Following the first nutrient pulse, we found clear evidence of a critical transition only within the pulsed low coupling pond with no evidence of a

418 critical transition in the paired reference pond. This suggests that the chlorophyll-*a* response was
419 due to the nutrient addition rather than stochastic environmental dynamics. The critical transition
420 following the first nutrient pulse likely influenced the rapid response of chlorophyll-*a* to the
421 second nutrient pulse within the pulsed low coupling pond, as a critical transition may indicate
422 an ecosystem is more vulnerable to major changes induced by small perturbations (Taranu et al.,
423 2018). There was no evidence of a critical transition following the second nutrient pulse in any of
424 the pulsed ponds, though there was evidence of a critical transition in the reference low and high
425 coupling ponds. However, the critical transition in the reference ponds was likely related to an
426 extreme storm event (derecho) that occurred on DOY 223 discussed below.

427 Within the experimental ponds, there were several factors that produced uncertainty we
428 were unable to control. There was enhanced zooplanktivory due to the unknown presence of
429 remnant bigmouth buffalo *(Ictiobus cyprinellus*) in the pulsed low coupling pond (n=10) and
430 reference high coupling pond (n=2) from an ecosystem experiment the previous year (Wilkinson
431 et al. 2022). Bigmouth buffalo are endemic planktivores and may have contributed to the lower
432 zooplankton biomass in the pulsed low coupling pond compared to the reference. It is also
433 possible bigmouth buffalo contributed to the chlorophyll-*a* response in the low coupling pond as
434 well as the evidence of a critical transition. However, bigmouth buffalo rely on zooplankton for
435 food, mainly copepods and large-bodied cladocerans; thus, it is unlikely that their presence
436 affected the degree of benthic-pelagic coupling as they are not generalist consumers (Starostka
437 and Applegate 1970, Adámek et al. 2003). All ponds, however, were subject to increased
438 zooplanktivory from larval bluegill and largemouth bass spawned during the study period and
439 both the reference and pulsed low coupling ponds had consistent zooplankton biomass dynamics.

440 The experimental ponds were also subjected to two unanticipated extreme weather events

441 that may have influenced ecosystem dynamics in addition to our nutrient pulse additions. First,
442 there was a five-day period of elevated surface water temperatures that occurred nine days after
443 the first nutrient pulse on DOY 185 – 190 (Appendix S1: Figure S5). The combination of
444 nutrients and elevated temperatures may have helped stimulate phytoplankton production
445 following the first nutrient pulse (Albright et al. 2022). This also led to the senescence of
446 macrophytes in the deeper portions of the pond in the pulsed treatments, but the floating
447 macrophytes which ringed the pond were unaffected. Elevated temperatures and macrophyte
448 senescence driving alterations in stratification dynamics likely affected metabolism estimates
449 (Cole et al. 2000, Hornbach et al. 2020), perhaps explaining why we did not observe stronger
450 responses. Second, as mentioned above, there was a derecho on DOY 223 that fully and violently
451 mixed the water columns of all the ponds (Albright et al. 2022), but the duration of effects was
452 short. It is likely the derecho caused nutrients or organic matter to be released by the alteration of
453 stratification via mixing (Lehman 2014, Salmaso et al. 2018), which may have stimulated
454 primary production in all ponds, including the reference ponds. This process may have resulted
455 in the small increase in phytoplankton, GPP, and R in all ponds near the end of the experiment,
456 as well as contributed to the critical transitions in the low and high coupling reference ponds as
457 mentioned previously. Even so, the increase in primary production was not significant.
458 Benthic-pelagic coupling is increasingly recognized as an important component of food
459 web structure within aquatic ecosystems (McMeans et al. 2016). Here, we demonstrate
460 empirically that, even in highly spatially constrained ecosystems, coupling between benthic and
461 pelagic energy pathways produced increased resistance and resilience of the ecosystems to
462 nutrient pulses. While other studies have demonstrated the importance of benthic-pelagic
463 coupling, our study provides empirical and mechanistic evidence that greater benthic-pelagic

coupling could be a key target for lake management programs to increase ecosystem resistance and resilience to increasingly frequent and severe disturbances. Preserving or enhancing benthic-pelagic coupling is vital for aquatic ecosystems, especially as coupling and energy flow can be adversely affected by increasing eutrophication (Wang et al. 2020). However, how benthic-pelagic coupling may interact with fishes that substantially affect nutrient cycling, both native (e.g., gizzard shad; Schaus et al. 1997) and non-native (e.g., common carp; (Weber and Brown 2011), should be explored further. Here, we provide further empirical support that biodiversity and the architecture of species interactions within a food web is a key ecosystem property that makes ecosystems more resistant and resilient to environmental change and must be preserved.

Acknowledgements: We thank Michael Tarnow, Mathew Kremer, Elena Sandry, Quin Shingai, Ellen Albright, Sofia Ferrer, and Kayleigh Winston, for assistance with sample collection and analysis, Martin Simonson, and the Weber Lab for collecting fish, and Cal Buelo and Jonathan Walter for their assistance with data analysis. This research was supported by the Iowa Water Center's Graduate Student Supplemental Research Competition. Butts was supported by the National Science Foundation Graduate Research Fellowship Program (DGE-1747503) and Wilkinson was supported by NSF # 2200391. Any opinions, findings, and conclusions or recommendations expressed in this material are those of the authors and do not necessarily reflect the views of the National Science Foundation.

Conflict of Interest: The authors declare no conflict of interest.

REFERENCES

Adámek, Z., I. Sukop, P. M. Rendón, and J. Kouřil. 2003. Food competition between 2+ tench (Tinca tinca L.), common carp (Cyprinus carpio L.) and bigmouth buffalo (Ictiobus cyprinellus Val.) in pond polyculture. Journal of Applied Ichthyology 19:165-169.

Albright, E. A., R. Ladwig, and G. M. Wilkinson. 2022. Macrophyte-hydrodynamic interactions mediate stratification and dissolved oxygen dynamics in ponds. EarthArXiV.

Baustian, M. M., G. J. a. Hansen, A. de Kluijver, K. Robinson, E. N. Henry, L. B. Knoll, K. C. Rose, and C. C. Carey. 2014. Linking the bottom to the top in aquatic ecosystems: mechanisms and stressors of benthic-pelagic coupling. Pages 25-47 Eco-DAS X Symposium Proceedings.

Burnham, K. P., and D. R. Anderson. 2004. Multimodel inference: Understanding AIC and BIC in model selection. Sociological Methods and Research 33:261-304.

Calizza, E., L. Rossi, G. Careddu, S. S. Caputi, and M. L. Costantini. 2019. Species richness and vulnerability to disturbance propagation in real food webs. Scientific Reports 9:19331.

Carey, M. P., and D. H. Wahl. 2010. Interactions of multiple predators with different foraging modes in an aquatic food web. Oecologia 162:443-452.

Carlander, K. 1977. Biomass, Production, and Yields of Walleye (Stizostedion vitreum vitreum) and Yellow Perch (Perca flavescens) in North American Lakes. Journal of Fisheries Research Board of Canada 34:1602-1612.

Carmichael, W. W., and G. L. Boyer. 2016. Health impacts from cyanobacteria harmful algae blooms: Implications for the North American Great Lakes. Harmful Algae 54: 194-212.

Carpenter, S. R., E. G. Booth, and C. J. Kucharik. 2018. Extreme precipitation and phosphorus loads from two agricultural watersheds. Limnology and Oceanography 63:1221-1233.

508 Cole, J. J., M. L. Pace, S. R. Carpenter, and J. F. Kitchell. 2000. Persistence of net heterotrophy
509 in lakes during nutrient addition and food web manipulations. Limnology and
510 Oceanography 45:1718-1730.
511 Cottingham, K., and D. Schindler. 2000. Effects of grazers community structure on
512 phytoplankton response to nutrient pulses. Ecology 81:183-200.
513 Duffy, W. G. 1998. Population dynamics, production, and prey consumption of fathead minnows
514 (Pimephales promelas) in prairie wetlands: a bioenergetics approach. Canadian Journal of
515 Fisheries and Aquatic Sciences 54:15-27.
516 Ho, J. C., and A. M. Michalak. 2020. Exploring temperature and precipitation impacts on
517 harmful algal blooms across continental U.S. lakes. Limnology and Oceanography 65:992-
518 1009.
519 Hodgson, J. Y., and J. R. Hodgson. 2000. Exploring optimal foraging by largemouth bass
520 (Micropterus salmoides) from three experimental lakes. Verhandlungen des Internationalen
521 Verein Limnologie 27:1-6.
522 Hornbach, D. J., E. G. Schilling, and H. Kundel. 2020. Ecosystem metabolism in small ponds:
523 The eects of floating-leaved macrophytes. Water (Switzerland) 12:1-25.
524 Hughes, T. P., J. T. Kerry, A. H. Baird, S. R. Connolly, A. Dietzel, C. M. Eakin, S. F. Heron, A. S.
525 Hoey, M. O. Hoogenboom, G. Liu, M. J. McWilliam, R. J. Pears, M. S. Pratchett, W. J.
526 Skirving, J. S. Stella, and G. Torda. 2018. Global warming transforms coral reef
527 assemblages. Nature 556:492-496.
528 Hurvich, C. M., and C. -L Tsai. 1993. A Corrected Akaike Information Criterion for Vector
529 Autoregressive Model Selection. Journal of Time Series Analysis 14:271-279.

530 Ives, A. R., and V. Dakos. 2012. Detecting dynamical changes in nonlinear time series using
531 locally linear state-space models. Ecosphere 3:art58.
532 Jackson, J., V. Resh, D. Batzer, R. Merritt, and K. Cummins. 2019. Sampling Aquatic Insects:
533 Collection Devices, Statistical Considerations, and Rearing Procedures. Pages 17–42 *in* R.
534 Merritt, K. Cummins, and M. Berg, editors. An Introduction to the Aquatic Insects of North
535 America. Fifth edition. Kendall Hunt Publishing Company, Dubuque, IA.
536 Joosse, P. J., and D. B. Baker. 2011. Context for re-evaluating agricultural source phosphorus
537 loadings to the great lakes. Canadian Journal of Soil Science 91:317-327.
538 Lehman, J. T. 2014. Understanding the role of induced mixing for management of nuisance algal
539 blooms in an urbanized reservoir. Lake and Reservoir Management 30:63-71.
540 Lürling, M., M. M. Mello, F. van Oosterhout, L. de S. Domis, and M. M. Marinho. 2018.
541 Response of natural cyanobacteria and algae assemblages to a nutrient pulse and elevated
542 temperature. Frontiers in Microbiology 9:1-14.
543 McCann, K., A. Hastings, and G. Huxel. 1998. Weak trophic interactions and the balance of
544 nature. Nature 395:794-798.
545 McMeans, B. C., K. S. McCann, T. D. Tunney, A. T. Fisk, A. M. Muir, N. Lester, B. Shuter, and
546 N. Rooney. 2016. The adaptive capacity of lake food webs: From individuals to ecosystems.
547 Ecological Monographs 86:4-19.
548 Mougi, A. 2020. Coupling of green and brown food webs and ecosystem stability. Ecology and
549 Evolution:1-8.
550 Polazzo, F., T. As, I. Marina, M. Crettaz-Minaglia, and A. Rico. 2022. Food web rewiring drives
551 long-term compositional differences and late-disturbance interactions at the community
552 level. Proceedings of the National Academy of Sciences 119:e2117364119.

553 Prein, A. F., C. Liu, K. Ikeda, S. B. Trier, R. M. Rasmussen, G. J. Holland, and M. P. Clark.
554 2017. Increased rainfall volume from future convective storms in the US. Nature Climate
555 Change 7:880–884.
556 R Core Team. 2022. R: A language and environment for statistical computing. R Foundation for
557 Statistical Computing, Vienna, Austria.
558 Rooney, N., and K. S. McCann. 2012. Integrating food web diversity, structure and stability.
559 Trends in Ecology and Evolution 27:40-46.
560 Rose, K. C., L. A. Winslow, J. S. Read, E. K. Read, C. T. Solomon, R. Adrian, and P. C. Hanson.
561 2014. Improving the precision of lake ecosystem metabolism estimates by identifying
562 predictors of model uncertainty. Limnology and Oceanography: Methods 12:303-312.
563 Sabo, R. D., C. M. Clark, D. A. Gibbs, G. S. Metson, M. J. Todd, S. D. LeDuc, D. Greiner, M.
564 M. Fry, R. Polinsky, Q. Yang, H. Tian, and J. E. Compton. 2021. Phosphorus Inventory for
565 the Conterminous United States (2002–2012). Journal of Geophysical Research:
566 Biogeosciences 126.
567 Salmaso, N., A. Boscaini, C. Capelli, and L. Cerasino. 2018. Ongoing ecological shifts in a large
568 lake are driven by climate change and eutrophication: evidence from a three-decade study in
569 Lake Garda. Hydrobiologia 824:177-195.
570 Schaus, M. H., M. J. Vanni, M. T. Wissing, M. T. Brmigan, J. E. Garvey, and R. A. Stein. 1997.
571 Nitrogen and Phosphorus Excretion by Detritivorous Gizzard Shad in a Reservoir
572 Ecosystem. Limnology and Oceanography:1386-1397.
573 Scheffer, M., and Carpenter. 2003. Catastrophic regime shifts in ecosystems: linking theory to
574 observation. Trends in Ecology and Evolution 18:648-656.

575 Seneviratne, S., X. Zhang, M. Adnan, W. Badi, C. Dereczynski, A. Di Luca, S. Ghosh, I.
576 Iskandar, J. Kossin, S. Lewis, F. Otto, I. Pinto, M. Satoh, S. M. Vicente-Serrano, M.
577 Wehner, and B. Zhou. 2021. Weather and Climate Extreme Events in a Changing Climate.
578 Pages 1513–1766 *in* V. Masson-Delmotte, P. Zhai, A. Pirani, S. L. Connors, C. Péan, S.
579 Berger, N. Caud, Y. Chen, L. Goldfarb, M. I. Gomis, M. Huang, K. Leitzell, E. Lonnoy, J.
580 B. R. Matthews, T. K. Maycock, T. Waterfield, ,O. Yelekçi, R. Yu, and B. Zhou, editors.
581 Climate Change 2021: The Physical Science Basis. Contribution of Working Group I to the
582 Sixth Assessment Report of the Intergovernmental Panel on Climate Change. Cambridge
583 University Press, Cambridge, United Kingdom and New York, NY, USA.
584 Starostka, V. J., and R. L. Applegate. 1970. Food Selectivity of Bigmouth Buffalo , Ictiobus
585 cyprinellus , in Lake Poinsett , South Dakota. Transactions of the American Fisheries
586 Society 99:571-576.
587 Stockwell, J. D., J. P. Doubek, R. Adrian, O. Anneville, C. C. Carey, L. Carvalho, L. N. De
588 Senerpont Domis, G. Dur, M. A. Frassl, H.-P. Grossart, B. W. Ibelings, M. J. Lajeunesse, A.
589 M. Lewandowska, M. E. Llames, S.-I. S. Matsuzaki, E. R. Nodine, P. Nõges, V. P. Patil, F.
590 Pomati, K. Rinke, L. G. Rudstam, J. A. Rusak, N. Salmaso, C. T. Seltmann, D. Straile, S. J.
591 Thackeray, W. Thiery, P. Urrutia-Cordero, P. Venail, P. Verburg, R. I. Woolway, T. Zohary,
592 M. R. Andersen, R. Bhattacharya, J. Hejzlar, N. Janatian, A. T. N. K. Kpodonu, T. J.
593 Williamson, and H. L. Wilson. 2020. Storm impacts on phytoplankton community dynamics
594 in lakes. Global Change Biology:1–27.
595 Taranu, Z. E., S. R. Carpenter, V. Frossard, J. P. Jenny, Z. Thomas, J. C. Vermaire, and M. E.
596 Perga. 2018. Can we detect ecosystem critical transitions and signals of changing resilience
597 from paleo-ecological records? Ecosphere 9.

598 Turner, M. G., W. J. Calder, G. S. Cumming, T. P. Hughes, A. Jentsch, S. L. LaDeau, T. M.
599 Lenton, B. N. Shuman, M. R. Turetsky, Z. Ratajczak, J. W. Williams, A. P. Williams, and S.
600 R. Carpenter. 2020. Climate change, ecosystems and abrupt change: Science priorities.
601 Philosophical Transactions of the Royal Society B: Biological Sciences 375.
602 Tyson, J. T., and R. L. Knight. 2001. Response of Yellow Perch to Changes in the Benthic
603 Invertebrate Community of Western Lake Erie. Transactions of the American Fisheries
604 Society 130:766-782.
605 Vadeboncoeur, Y., D. Lodge, and S. Carpenter. 2001. Whole-lake fertilization effects on
606 distribution of primary production between benthic and pelagic habitats. Ecology 82:1065-
607 1077.
608 Vadeboncoeur, Y., K. S. McCann, M. J. Vander Zanden, and J. B. Rasmussen. 2005. Effects of
609 multi-chain omnivory on the strength of trophic control in lakes. Ecosystems 8:682–693.
610 Vadeboncoeur, Y., M. J. Vander Zanden, and D. M. Lodge. 2002. Putting the Lake Back
611 Together : Reintegrating Benthic Pathways into Lake Food Web Models 52.
612 Vanni, M. J., W. H. Renwick, J. L. Headworth, J. D. Auch, and M. H. Schaus. 2001. Dissolved
613 and particulate nutrient flux from three adjacent agricultural watersheds: A five-year study.
614 Biogeochemistry 54:85–114.
615 Walter, J. A., C. D. Buelo, A. F. Besterman, S. J. Tassone, J. W. Atkins, and M. L. Pace. 2022. An
616 algorithm for detecting and quantifying disturbance and recovery in high-frequency time
617 series. Limnology and Oceanography: Methods 20:338–349.
618 Walter, J., and C. Buelo. 2022. jonathan-walter/disturbhf: lno-methods paper version (v1.0.0).
619 Zenodo.

620 Wang, S. C., X. Liu, Y. Liu, and H. Wang. 2020. Benthic-pelagic coupling in lake energetic food
621 webs. Ecological Modelling 417:108928.
622 Ward, C. L., and K. S. McCann. 2017. A mechanistic theory for aquatic food chain length.
623 Nature communications 8:2028.
624 Weber, M. J., and M. L. Brown. 2011. Relationships among invasive common carp, native fishes
625 and physicochemical characteristics in upper Midwest (USA) lakes. Ecology of Freshwater
626 Fish 20:270-278.
627 Werner, E. E., and D. J. Hall. 1988. Ontogenetic habitat shifts in bluegill: the foraging rate-
628 predation risk trade-off. Ecology 69:1352-1366.
629 Wilkinson, G., T. Butts, E. Sandry, M. Simonson, and M. Weber. 2022. Experimental evaluation
630 of the effects of bigmouth buffalo (Ictiobus cyprinellus) density on shallow lake
631 ecosystems. Earth Arxiv.
632 Wojcik, L. A., R. Ceulemans, and U. Gaedke. 2021. Functional diversity buffers the effects of a
633 pulse perturbation on the dynamics of tritrophic food webs. Ecology and Evolution
634 11:15639-15663.
635 Vander Zanden, M. J., T. E. Essington, and Y. Vadeboncoeur. 2005. Is pelagic top-down control
636 in lakes augmented by benthic energy pathways? Canadian Journal of Fisheries and Aquatic
637 Sciences 62:1422-1431.
638 Vander Zanden, M. J., and Y. Vadeboncoeur. 2002. Fishes as integrators of benthic and pelagic
639 food webs in lakes. Ecology 83:2152-2161.
640 Zanette, L. Y., and M. Clinchy. 2019. Ecology of fear. Current Biology 29:R309-R313.

TABLES

Table 1. Mean (standard deviation) of water quality metrics in micrograms per liter (µg L^{-1}) or milligrams per liter (mg L^{-1}) (n=46 – 47) along with the added fish biomass for all ponds (n.p. = not present) in kilograms per hectare (kg ha^{-1}). Pulsed refers to ponds that received the two nutrient additions and reference are ponds that did not receive nutrients.

	Low Coupling		**Intermediate**		**High Coupling**	
Variable	***Pulsed***	***Reference***	***Pulsed***	***Reference***	***Pulsed***	***Reference***
Total P (µg L^{-1})	39 (11)	47 (22)	70 (47)	51 (36)	35 (12)	46 (12)
Total N (mg L^{-1})	0.39 (0.15)	0.41 (0.15)	0.41 (0.20)	0.42 (0.18)	0.39 (0.16)	0.36 (0.15)
Soluble P (µg L^{-1})	3.9 (0)	4.2 (0.94)	4.0 (0.30)	5.3 (2.5)	3.9 (0)	7.2 (5.2)
Nitrate – N (mg L^{-1})	0.13 (0.070)	0.12 (0.070)	0.13 (0.082)	0.14 (0.077)	0.13 (0.073)	0.13 (0.081)
Ammonium – N (mg L^{-1})	0.024 (0.023)	0.022 (0.027)	0.016 (0.019)	0.013 (0.017)	0.015 (0.016)	0.024 (0.029)
Bluegill (kg ha^{-1})	21	20	21	21	20	21
Yellow Perch (kg ha^{-1})	20	20	20	19	19	20
Largemouth Bass (kg ha^{-1})	n.p.	n.p.	24	26	23	30
Fathead Minnow (kg ha^{-1})	n.p.	n.p.	n.p.	n.p.	9.0	9.0

646 **Table 2.** Response and recovery times of experimental ponds based on a response threshold of
647 2.0 and recovery threshold of 0.5. If a response did not occur, it was listed as not detected (n.d.),
648 and therefore a recovery could not be recorded. The days to response is the difference between
649 the day when a response was triggered and the addition of a nutrient pulse. The days to recover is
650 the difference between the day a response was detected and the day the pond recovered.

651

		Chlorophyll-*a*		Gross Primary Production		Respiration	
	Nutrient Pulse	***Days to Respond***	***Days to Recover***	***Days to Respond***	***Days to Recover***	***Days to Respond***	***Days to Recover***
Low Coupling	Pulse 1	24	5	n.d.	--	n.d.	--
	Pulse 2	8	22	n.d.	--	n.d.	--
Intermediate Coupling	Pulse 1	18	23	11	11	n.d.	--
	Pulse 2	20	n.d.	21	5	21	4
High Coupling	Pulse 1	n.d.	--	n.d.	--	n.d.	--
	Pulse 2	n.d.	--	n.d.	--	n.d.	--

652

653

654 **FIGURE CAPTIONS**

655 **Figure 1.** Conceptual diagram of the experimental design of the six pond ecosystems. Dark
656 arrows indicate benthic food chain pathways and light arrows indicate pelagic food chain
657 pathways. Text labels denote common names of organisms represented. This diagram does not
658 represent the actual layout of the reference and pulsed ponds which were randomized.
659
660 **Figure 2.** Time series of zooplankton biomass in micrograms per liter (µg L^{-1}, A - C),
661 macroinvertebrate density in number per square meter (# m^{-2}, D - F), and periphyton areal
662 biomass in micrograms per square centimeter (µg cm^{-2}, G - I). The dark colored line indicates the
663 disturbed time series, and the gray line indicates the reference time series.
664
665 **Figure 3.** Dynamics of chlorophyll-*a* in micrograms per liter (µg L^{-1}, A - C), gross primary
666 production (GPP, D - F), respiration (absolute value, |R|, G - I), and net ecosystem production
667 (NEP, J - L) in milligrams of oxygen per liter per day (mg O_2 L^{-1} d^{-1}). Data were fitted with
668 LOESS regression analysis (10% span) for visualization purposes, standard error is defined by
669 the shaded region. The dark colored line indicates the disturbed time series, and the dark gray
670 line indicates the reference time series. In all figures, the dashed vertical line denotes the nutrient
671 pulses on day of year 176 and 211 and the horizontal line at zero (panels J - L) shows whether
672 the ecosystem was autotrophic (NEP > 0) or heterotrophic (NEP < 0).
673
674 **Figure 4.** Time series of modified Z-scores of chlorophyll-*a* concentrations (A - C), gross
675 primary production (D - F), respiration (G - I), and net ecosystem production (J - L) generated by
676 the response detection algorithm (Walter et al. 2022). In all figures, the thick horizontal line

677 denotes the response threshold, and the thin horizontal line denotes the recovery threshold. The
678 recovery threshold cannot be documented until a disturbance has occurred. The dashed vertical
679 lines indicate when the nutrient pulses were delivered to each pond.
680
681 **Figure 5.** The eigenvalues (dark lines) and their bootstrapped standard error (shaded polygons)
682 of chlorophyll-*a* time series from ponds that received nutrient pulses (A-C) and reference ponds
683 (D-F). In all figures, the dashed vertical line denotes the nutrient pulses and the horizontal
684 dashed line at 1 is the threshold by which eigenvalues must cross above from below to be
685 considered a critical transition.
686

687 **FIGURES**

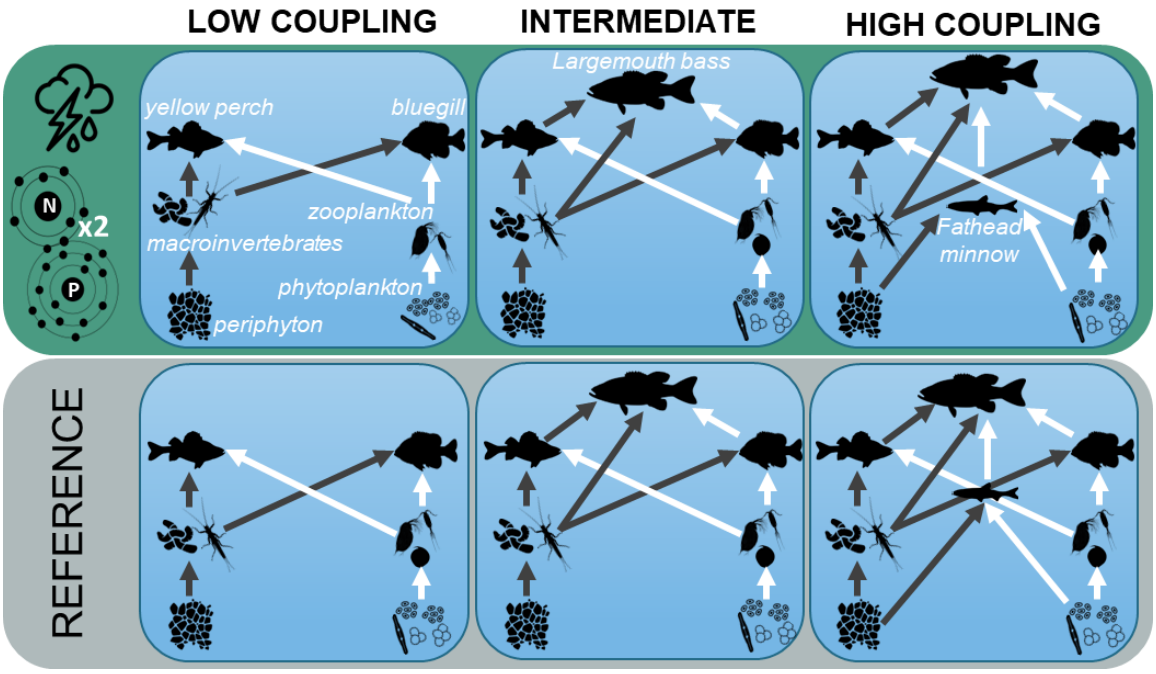

688
689 **Figure 1.**

690

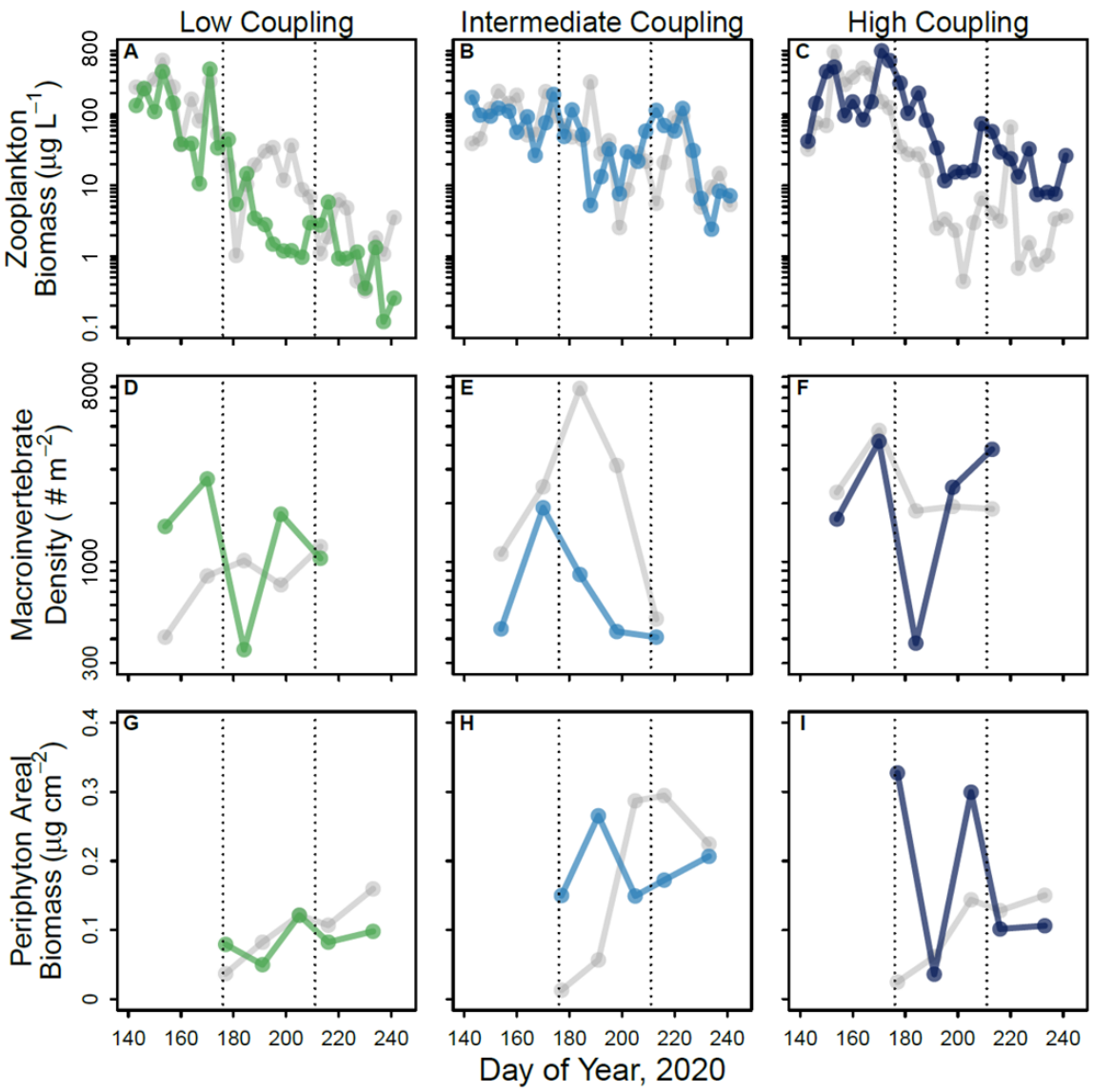

691
692 **Figure 2.**
693

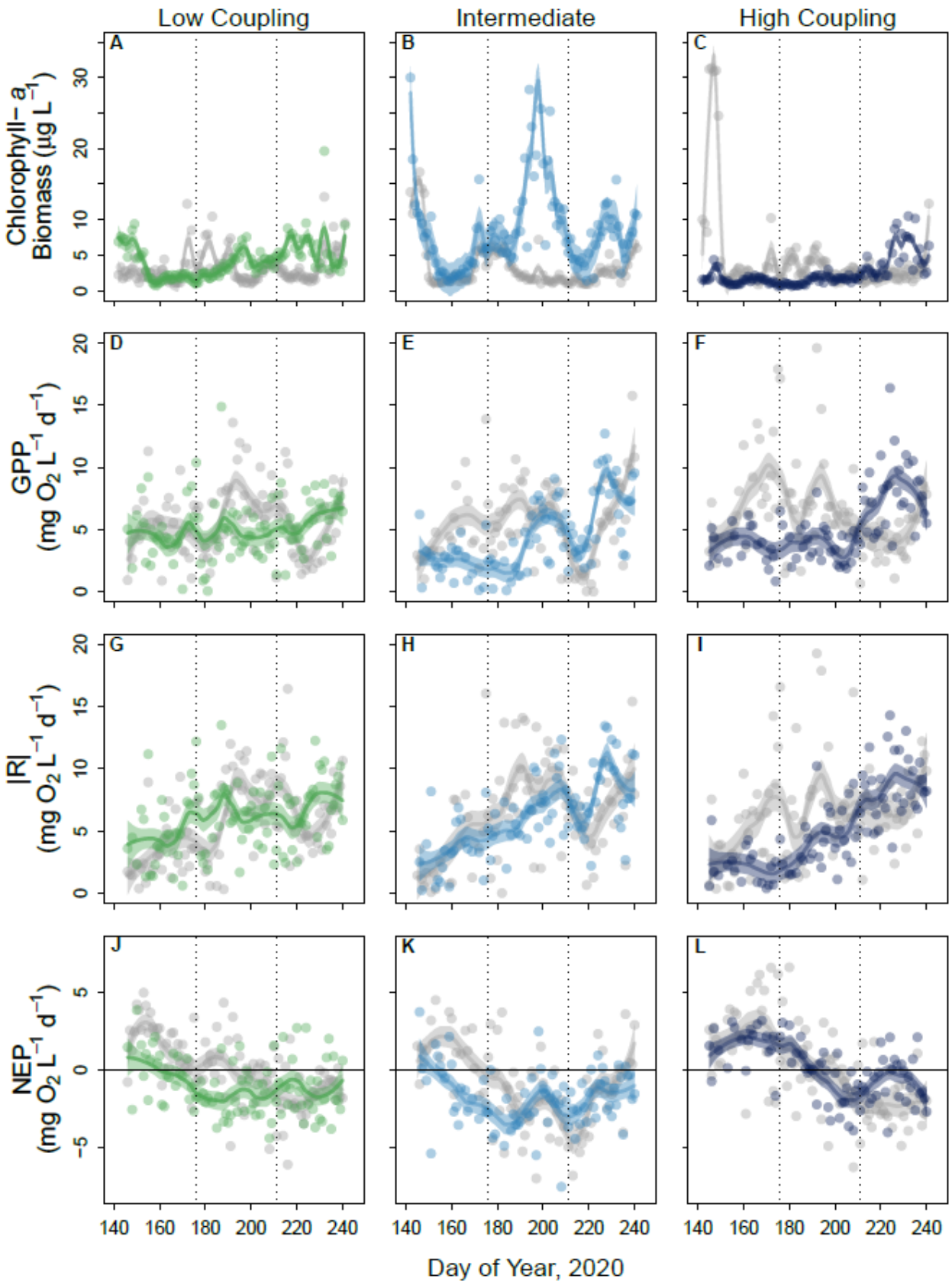

694
695 **Figure 3.**

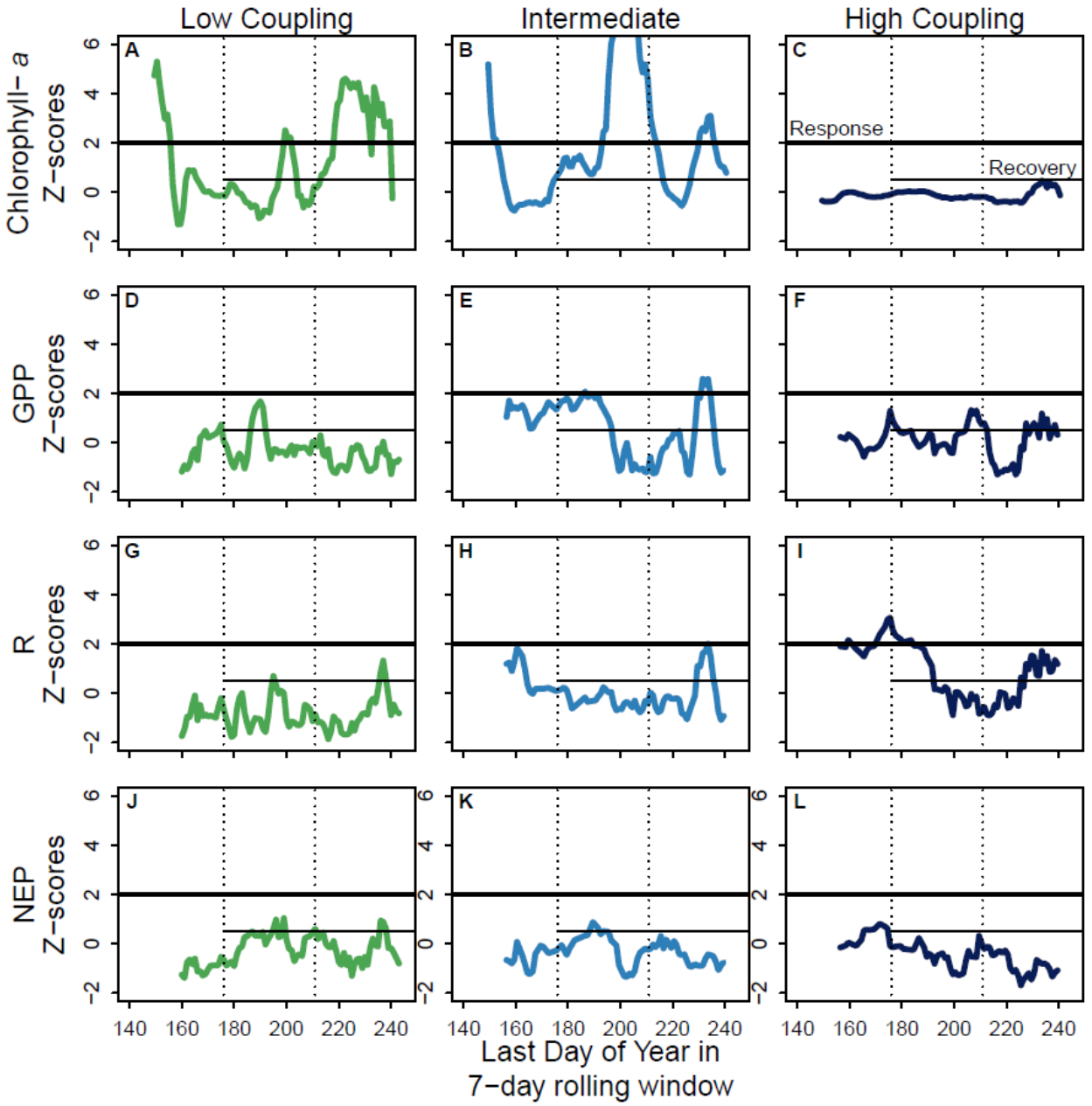
Low Coupling
Intermediate
High Coupling
Chlorophyll- a Z-scores
GPP Z-scores
R Z-scores
NEP Z-scores
A
B
C
D
E
F
G
H
I
J
K
L
Response
Recovery
-2
0
2
4
6
140
160
180
200
220
240
Last Day of Year in 7-day rolling window

Figure 4.

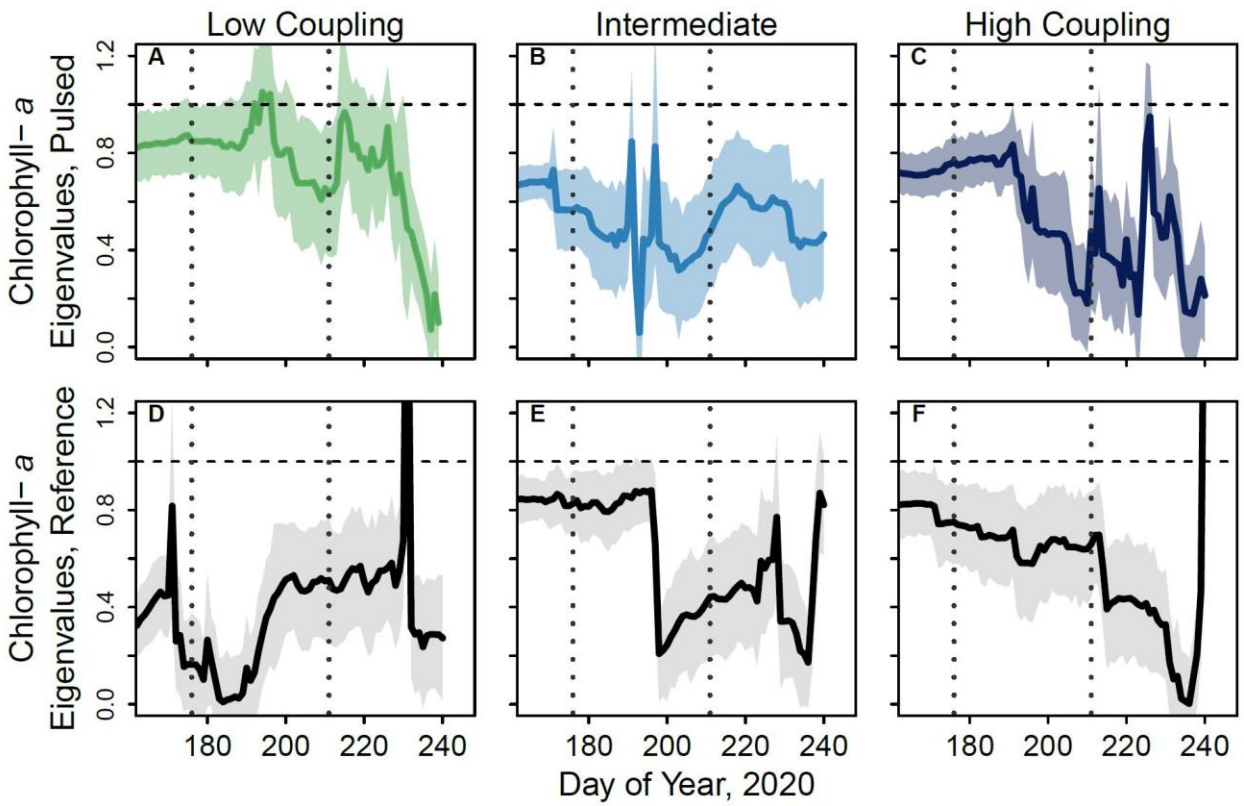
Low Coupling
Intermediate
High Coupling
A
B
C
D
E
F
Chlorophyll– a
Eigenvalues, Pulsed
Chlorophyll– a
Eigenvalues, Reference
0.0
0.4
0.8
1.2
180
200
220
240
Day of Year, 2020

Figure 5.

Appendix S1 for
Experimental evaluation of aquatic ecosystem resistance and resilience to episodic nutrient loading

Tyler J. Butts, Robert A. Johnson, Michael J. Weber, Grace M. Wilkinson

SUPPLEMENTAL METHODS

Periphyton

For periphyton, a modified Hester-Dendy sampler (173.28 cm^2) was deployed for two-week periods in each pond and areal chlorophyll-*a* was measured based on analysis of the biomass that grew on the artificial substrate during the deployment. Periphyton was brushed, scraped, and rinsed off the substrate (0.017 m^2) with deionized water and diluted to a known volume in amber bottles before analysis (Jacoby et al. 1991, Carey and Wahl 2011). Samples from each pond were homogenized to loosen algal 'clumps' and filtered onto Whatman glass fiber filters (0.45 µm). Areal chlorophyll-*a* (µg/m^2) was measured via acetone extraction using sonication (Bidigare et al. 2005) and analyzed using fluorometry (EPA Method 445.0) on a Turner Designs Trilogy Fluorometer (Arar and Collins 1997, Childress et al. 1999, Turner Designs 2001).

Nutrients

Phosphorus was measured via the phosphomolybdenum blue method (EPA method 365.1 v2) and nitrogen was measured via second-derivative ultraviolet spectroscopy (Crumpton et al. 1992, Childress et al. 1999) using an HP 8435 Spectrophotometer. Total phosphorus and nitrogen samples underwent a persulfate digestion before analysis to transform all P- or N- containing compounds into dissolved forms.

Zooplankton

Zooplankton were identified using a Leica MZ8 stereomicroscope connected to Motic Images software in a 1 mL subsample. If less than 60 organisms were identified within the 1 mL subsample, another subsample was counted. Up to 25 individuals per taxon were measured per sample to calculate dry mass per liter using standard length-mass regressions (Dumont et al. 1975; McCauley 1984).

Macroinvertebrates

Macroinvertebrates were sampled using a stovepipe sampler that had a diameter of 0.3 m. To assist with identification, we added 0.1% Rose Bengal Dye to preserved macroinvertebrate samples. In the lab, macroinvertebrates were further sieved on a 500-µm pan sieve and individuals were removed and identified to the lowest possible order or family. A stereomicroscope was used to identify mollusks and insects to family. Leeches and oligochaetes were identified to class. This level of taxonomic resolution is sufficient to reflect community patterns (Bowman and Bailey 1997). Sorted individuals were then used to calculate taxon richness and density (number of individuals/m^2).

Dissolved Oxygen Data Cleaning

Dissolved oxygen (DO) concentration was measured every 30 minutes in the surface waters of each pond over the course of the 96-day experiment. Prior to calculating daily rates of ecosystem metabolism, DO data were inspected and cleaned to account for times when a change in DO concentration was likely a result of physical processes (e.g., vertical mixing) rather than biological production or respiration. We used a conservative threshold of a change of 2.0 mg DO L^{-1} to identify these times. All times when DO concentration decreased by 2.0 mg L^{-1} or more from the previous measurement (i.e., a 2.0 mg L^{-1} drop in 30 minutes) were flagged and removed along with the subsequent five measurements (three hours total). These three-hour periods were then backfilled via linear interpolation. The majority of days did not require any cleaning and backfilling of DO data. Out of 576 total days (96 per pond), 345 days did not have any flagged DO measurements, 144 days had one flagged measurement, 71 days had two flagged measurements, and only 16 days had three or more flagged measurements.

As described in the manuscript text, calculating daily rates of metabolism using the free-oxygen method can result in erroneous estimates (i.e., negative GPP, positive R), and any days for which calculations returned an erroneous estimate were removed prior to further analyses. This resulted in the removal of 62 days due to erroneous metabolism estimates (range 4 – 18 days across all ponds), 40 of which were from days that did not have any flagged and cleaned DO measurements.

SUPPLEMENTAL REFERENCES

Bowman, M. F., & Bailey, R. C. (1997). Does taxonomic resolution affect the multivariate description of the structure of freshwater benthic macroinvertebrate communities? *Canadian Journal of Fisheries and Aquatic Sciences*, *54*(8), 1802–1807. https://doi.org/10.1139/f97-085

Burnham, K. P., & Anderson, D. R. (2004). Multimodel inference: Understanding AIC and BIC in model selection. In *Sociological Methods and Research* (Vol. 33, Issue 2, pp. 261–304). https://doi.org/10.1177/0049124104268644

Dumont, H. J., van de Velde, I., & Dumont, S. (1975). The dry weight estimate of biomass in a selection of Cladocera, Copepoda and Rotifera from the plankton, periphyton and benthos of continental waters. *Oecologia*, *19*(1), 75–97. https://doi.org/10.1007/BF00377592

McCauley, E. (1984). The estimation of the abundance and biomass of zooplankton in samples. In J. Downing & F. Rigler (Eds.), *A manual on methods for the assessment of secondary productivity in fresh waters* (pp. 228–265). Blackwell Publishing Ltd.

Mikulyuk, A., Sharma, S., van Egeren, S., Erdmann, E., Nault, M. E., & Hauxwell, J. (2011). The relative role of environmental, spatial, and land-use patterns in explaining aquatic macrophyte community composition. *Canadian Journal of Fisheries and Aquatic Sciences*, *68*(10), 1778–1789. https://doi.org/10.1139/f2011-095

SUPPLEMENTAL TABLES

Table S1. Mass, in grams, of nitrogen and phosphorus added to the experimental research ponds for each nutrient pulse along with the percent increase in ambient phosphorus concentrations.

	NH_4NO_3	$NaH_2PO_4(H_2O)_2$	Ambient increase
Nutrient Pulse 1	21.36	3.33	3 %
Nutrient Pulse 2	45.01	7.02	5 %

Table S2. Akaike Information Criterion corrected for small sample size (AICc) of online dynamic linear autoregressive models of chlorophyll-*a* concentration for each experimental pond at optimal order (p) of 1 or 2.

	p = 1	p = 2	ΔAICc
Low Coupling – pulsed	359.38	356.51	2.87
Low Coupling – reference	426.81	457.05	30.24
Intermediate – pulsed	554.2	580.49	26.29
Intermediate – reference	321.31	327.75	6.44
High Coupling – pulsed	245.5	273.39	27.89
High Coupling – reference	401.88	403.55	1.67

Table S3. The number of individuals identified in the stomach contents of fish at the end of the experiment collected via gastric lavage grouped by taxonomic identity. Macrophytes included plant pieces and stems, miscellaneous eggs were mostly frog eggs but some fish eggs as well, and frog refers to adults. If individuals of a certain taxa were not identified, they were marked as not detected (n.d.).

		Bluegill	***Yellow Perch***	***Largemouth Bass***
Low Coupling	Zooplankton	32	6	--
	Macroinvertebrate	115	45	--
	Misc. Eggs	3	n.d.	--
	Macrophytes	16	8	--
	Larval fish	n.d.	11	--
	Frog	n.d.	n.d.	--
Intermediate	Zooplankton	11	n.d.	n.d.
	Macroinvertebrate	55	25	22
	Misc. Eggs	10	n.d.	n.d.
	Macrophytes	16	1	1
	Larval fish	n.d.	7	4
	Frog	n.d.	n.d.	n.d.
High Coupling	Zooplankton	11	2	n.d.
	Macroinvertebrate	72	35	6
	Misc. Eggs	1	--	n.d.
	Macrophytes	15	2	1
	Minnow	n.d.	2	1
	Larval fish	n.d.	n.d.	n.d.
	Frog	n.d.	n.d.	1

Table S4. Response detection algorithm results for chlorophyll-*a*, gross primary production, respiration, and net ecosystem production with three rolling window lengths: five days, seven days, and ten days. The days to respond quantifies the number of days following the first or second nutrient pulse that it took Z-scores to move above the response threshold (Z = 2.0). Days to recover quantifies the number of days, once the Z-scores passed the response threshold, to move below the recovery threshold (Z = 0.5).

			Chlorophyll-*a*		Gross Primary Production		Respiration	
	Window	***Nutrient Pulse***	***Days to Respond***	***Days to Recover***	***Days to Respond***	***Days to Recover***	***Days to Respond***	***Days to Recover***
Low Coupling	7 days	Pulse 1	24	5	n.d.	--	n.d.	--
	7 days	Pulse 2	8	22	n.d.	--	n.d.	--
Intermediate Coupling	7 days	Pulse 1	18	23	11	11	n.d.	--
	7 days	Pulse 2	20	n.d.	21	5	21	4
High Coupling	7 days	Pulse 1	n.d.	--	n.d.	--	n.d.	--
	7 days	Pulse 2	n.d.	--	n.d.	--	n.d.	--
Low Coupling	5 days	Pulse 1	24	4	9	5	n.d.	--
	5 days	Pulse 2	8	14	n.d.	--	n.d.	--
Intermediate Coupling	5 days	Pulse 1	18	22	18	22	n.d.	--
	5 days	Pulse 2	19	9	19	9	21	4
High Coupling	5 days	Pulse 1	n.d.	--	n.d.	--	n.d.	--
	5 days	Pulse 2	n.d.	--	n.d.	--	n.d.	--
Low Coupling	10 days	Pulse 1	25	6	n.d.	--	n.d.	--
	10 days	Pulse 2	8	n.d	n.d.	--	n.d.	--
Intermediate Coupling	10 days	Pulse 1	5	38	4	17	n.d.	--
	10 days	Pulse 2	19	n.d.	22	4	n.d.	--
High Coupling	10 days	Pulse 1	n.d.	--	n.d.	--	n.d.	--
	10 days	Pulse 2	n.d.	--	n.d.	--	21	--

SUPPLEMENTAL FIGURES

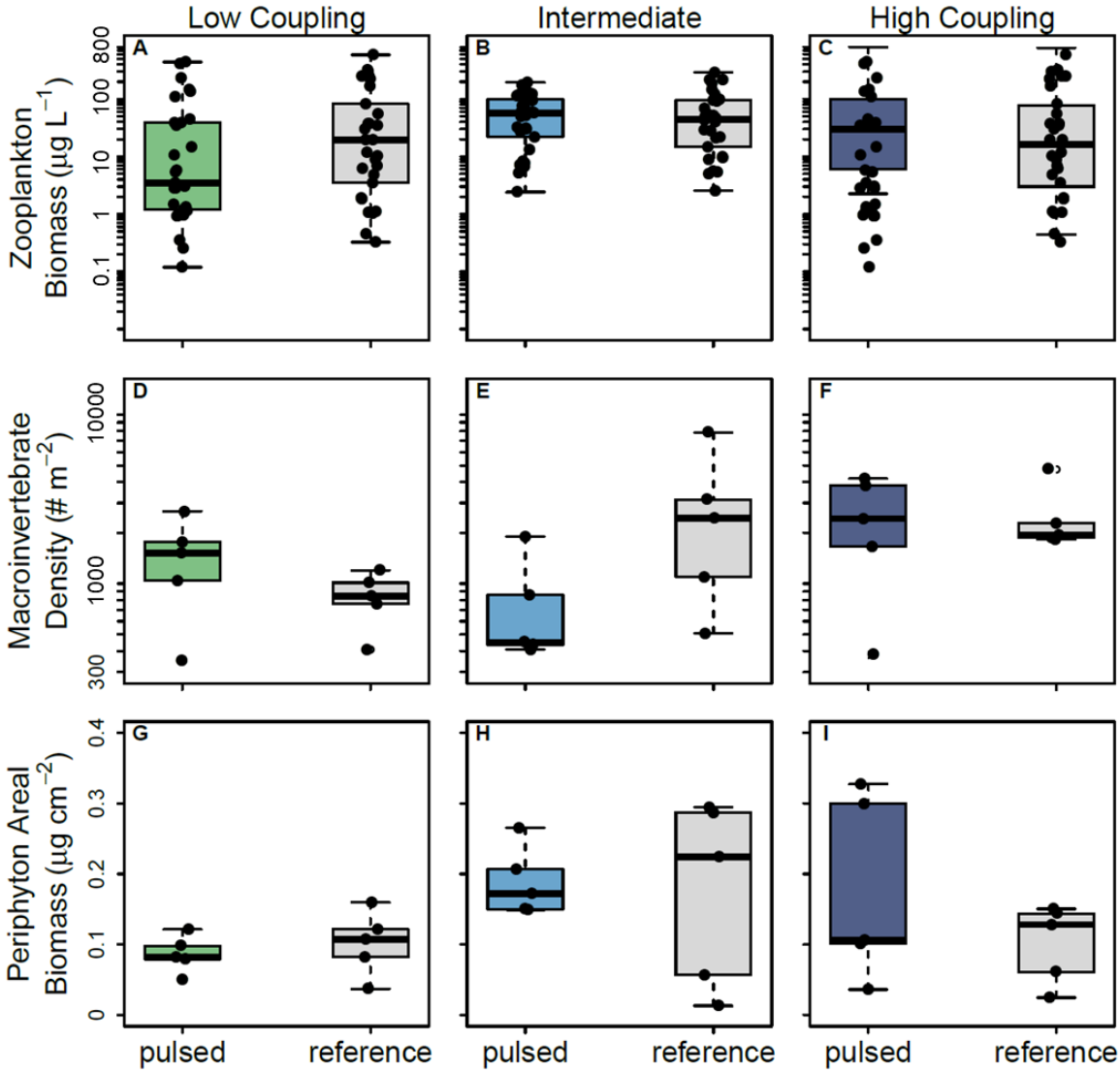

Figure S1. Food web context for experimental ponds over the course of the experiment for zooplankton biomass in micrograms per liter (µg L^{-1}; A - C), macroinvertebrate density in number per square meter (# m^{-2}; D – F), and periphyton areal biomass in micrograms per square centimeter (µg m^{-2}; G – I).

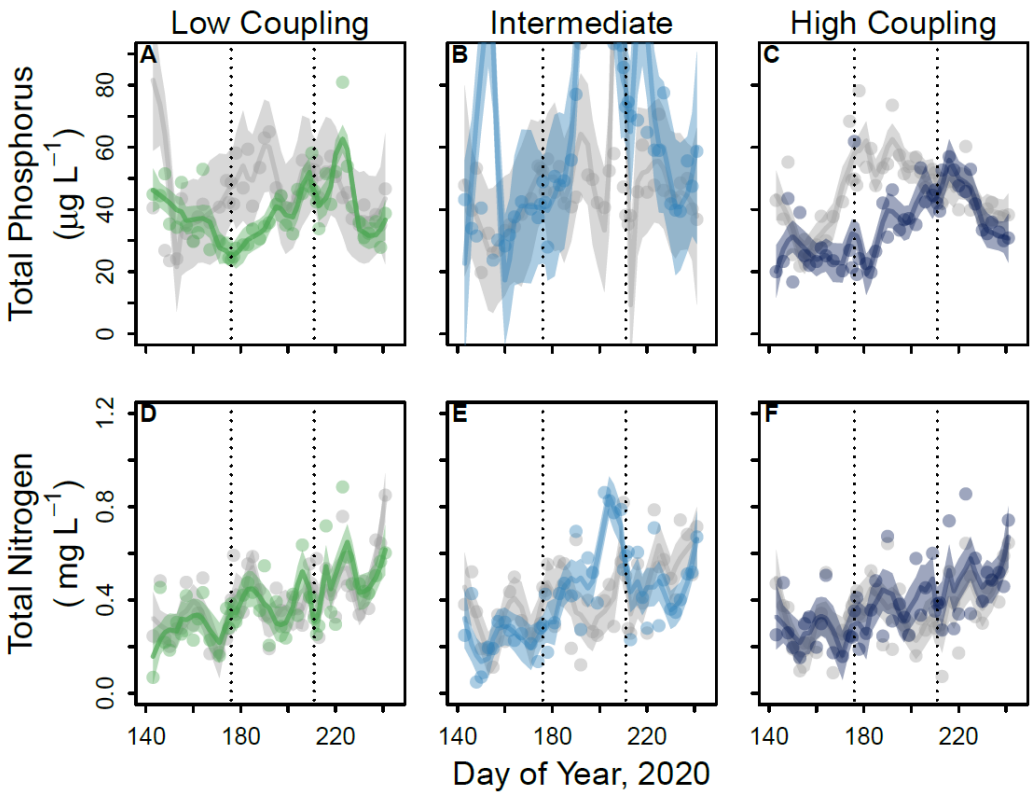

Figure S2. Time series of total nitrogen (mg L^{-1}) and phosphorus (µg L^{-1}). Data were fitted with LOESS regression analysis (20% span) for visualization purposes, error is defined by the shaded region. The dark colored line indicates the disturbed time series, and the gray line indicates the reference time series. In all figures, the dashed vertical line denotes the nutrient pulses on day of year 176 and 211.

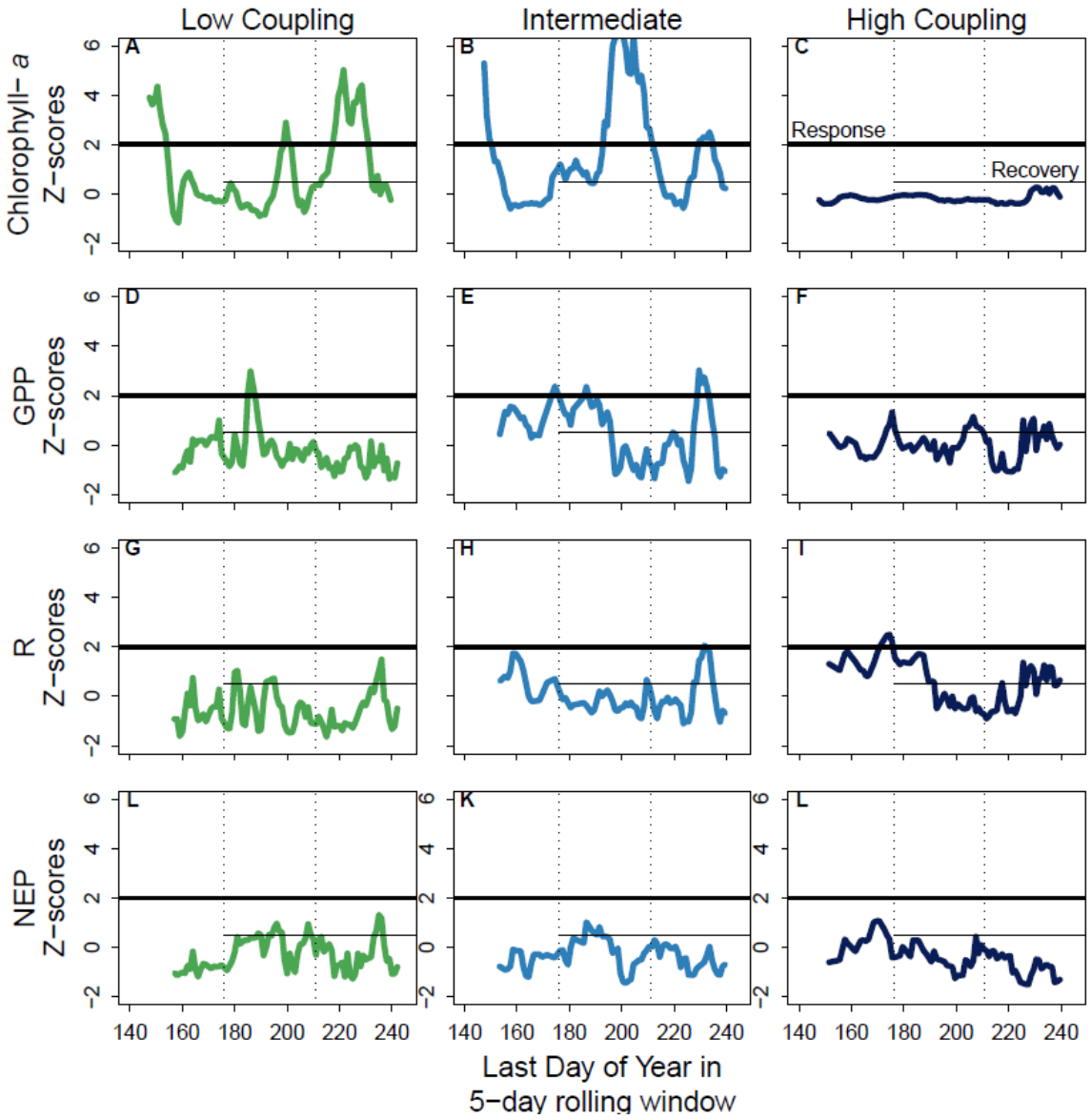

Figure S3. Time series of modified Z-scores of chlorophyll-*a* concentrations (A - C), gross primary production (D - F), respiration (G - I), and net ecosystem production (J - L) generated by the response detection algorithm (Walter et al. 2022) with a 5-day rolling window. In all figures the thick horizontal line denotes the response threshold, and the thin horizontal line denotes the recovery threshold. The recovery threshold can't be documented until a disturbance has occurred. The dashed vertical lines indicate when the nutrient pulses were delivered to each pond on day of year 176 and 211.

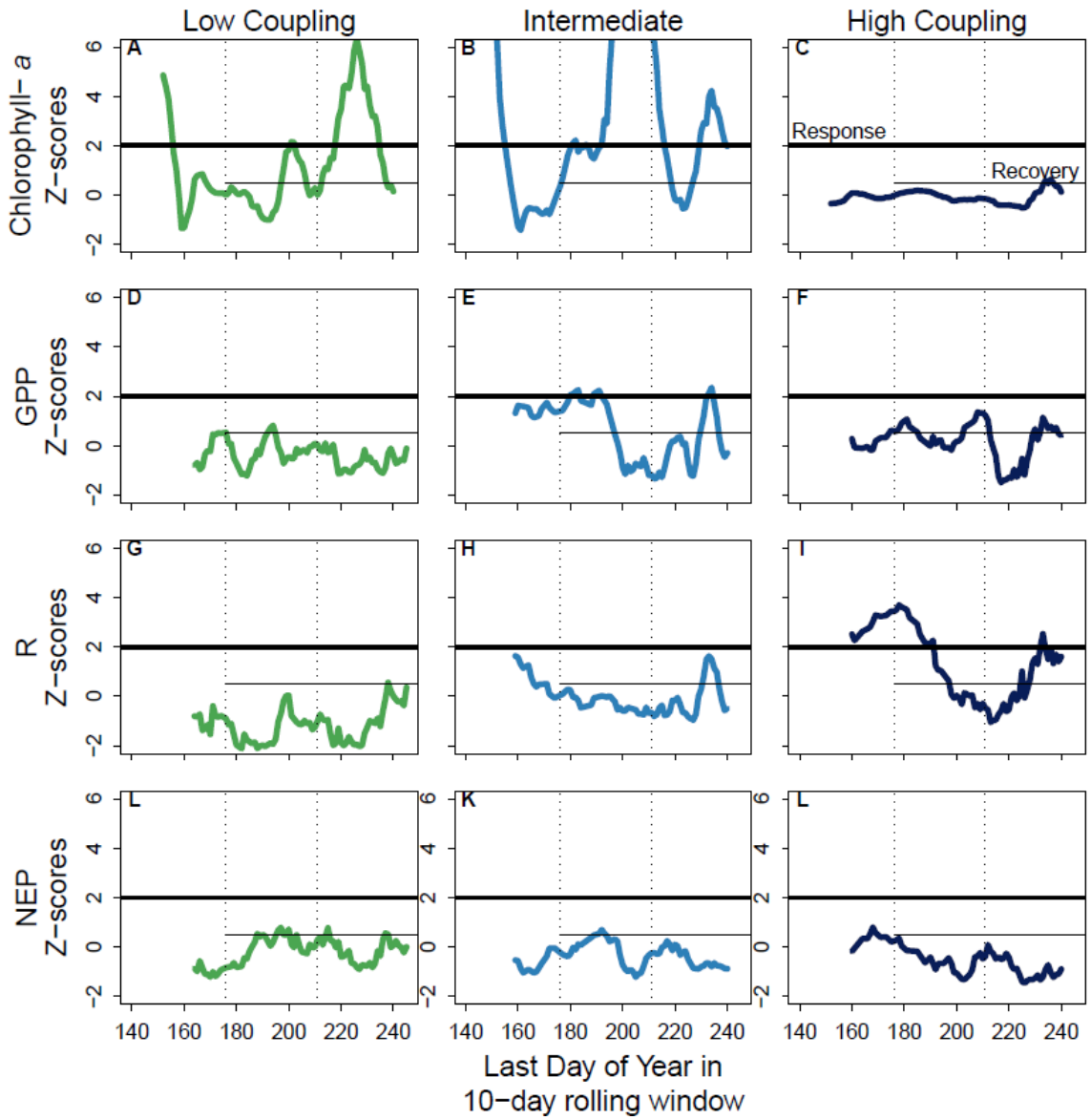

Figure S4. Time series of modified Z-scores of chlorophyll-*a* concentrations (A - C), gross primary production (D - F), respiration (G - I), and net ecosystem production (J - L) generated by the response detection algorithm (Walter et al. 2022) with a 10-day rolling window. In all figures the thick horizontal line denotes the response threshold, and the thin horizontal line denotes the recovery threshold. The recovery threshold can't be documented until a disturbance has occurred. The dashed vertical lines indicate when the nutrient pulses were delivered to each pond on day of year 176 and 211.

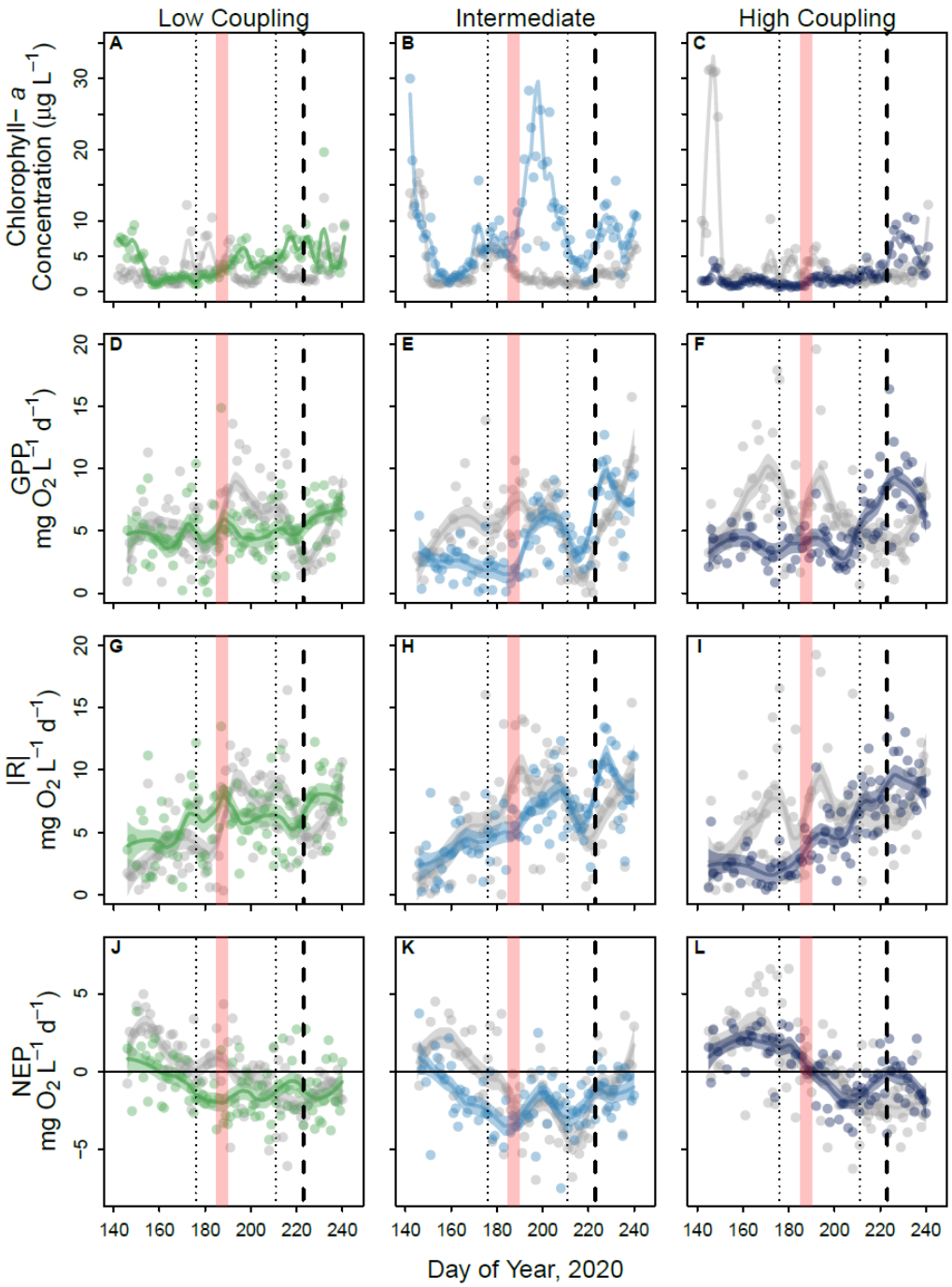

Figure S5. Dynamics of chlorophyll-*a* in micrograms per liter (µg L^{-1}), gross primary production (GPP), respiration (absolute value, |R|), and net ecosystem production (NEP) in milligrams of oxygen per liter per day (mg O_2 L^{-1} d^{-1}). Data were fitted with LOESS regression analysis for visualization purposes, error is defined by the shaded region. The dark colored line indicates the disturbed time series, and the gray line indicates the reference time series. In all figures, the dashed vertical line denotes the nutrient pulses on day of year 176 and 211 and the horizontal line at zero (J – L) shows whether the ecosystem was autotrophic (NEP > 0) or heterotrophic (NEP < 0). The five-day period of elevated surface water temperature is a red polygon, and the thick dashed vertical line indicates when the 2020 Iowa derecho occurred on DOY 223.